

## Angular distributions of electrons elastically scattered from H<sub>2</sub>

T. W. Shyn and W. E. Sharp

*Space Physics Research Laboratory, The University of Michigan, Ann Arbor, Michigan 48109*

(Received 30 October 1980)

Angular distributions of electrons elastically scattered from H<sub>2</sub> have been measured by a crossed-beam method. Energy and angular range covered were from 2.0 to 200 eV and from  $-96^\circ$  to  $+156^\circ$ , respectively. Comparison has been made with the previous measurements and theories. There is a good agreement above 100-eV incident energy between the previous measurements and theories and the present results, but below 100 eV considerable discrepancies exist between the previously reported results and the present measurements in the shape as well as in the magnitude of the angular distribution. The total cross sections of Golden *et al.* [D. E. Golden, H. W. Bandel, and J. A. Salerno, *Phys. Rev.* **146**, 40 (1966)] above 7 eV are smaller than the present results (pure elastic) by as much as 24%, and the results of Srivastava *et al.* [S. K. Srivastava, A. Chutjian, and S. Trajmar, *J. Chem. Phys.* **63**, 2659 (1975)] are also smaller than the present results by as much as 15%. The momentum-transfer cross section calculated directly from the present results of angular distribution show good agreement with those results derived from transport coefficients in swarm experiments by Frost and Phelps [L. S. Frost and A. V. Phelps, *Phys. Rev.* **127**, 1621 (1962)] and Crompton *et al.* [R. W. Crompton, D. K. Gibson, and A. I. McIntosh, *Aust. J. Phys.* **22**, 715 (1969)] below 7 eV, but not for results above 7 eV. The results of Srivastava *et al.* are in agreement within the experimental uncertainties above 10 eV.

### I. INTRODUCTION

The elastic scattering of electrons by the hydrogen molecule has been the focus of much theoretical effort this past decade. Recent review papers<sup>1,2</sup> have summarized most of the work. Much theoretical work<sup>3-9</sup> has been done using various models for the energy range above 100 and below 10 eV. A few papers<sup>10-12</sup> deal with the energy range between 10 and 100 eV. Laboratory measurements of the differential cross section (DCS) are more uncertain than the theoretical results. The measurements of Srivastava *et al.*<sup>13</sup> are the only independent absolute DCS of elastic scattering in the energy range of 3.0 to 75 eV. Linder and Schmidt<sup>14</sup> have measured the relative DCS from 0.3 to 15 eV then normalized them to the total cross section of Golden *et al.*<sup>15</sup> Fink *et al.*<sup>16</sup> and Wingerden *et al.*<sup>17</sup> have measured the DCS between 100 and 2000 eV.

There are differences of theoretical calculations (Hara,<sup>6</sup> Henry and Lane,<sup>9</sup> and Truhlar and Brandt<sup>11</sup>) for the DCS and total elastic-scattering cross section with the results of experiments by Srivastava *et al.*<sup>13</sup> and Golden *et al.*<sup>15</sup> below 10 eV. Also there is a significant disagreement between

the momentum-transfer cross sections derived from transport coefficients in swarm experiments by Frost and Phelps,<sup>18</sup> and Crompton *et al.*<sup>19</sup> and those of Srivastava *et al.* by a crossed-beam method. It is recognized that the elastic-scattering cross sections of H<sub>2</sub> are critical parameters necessary to calculate the energy deposition and energy transport in the atmospheres of Jupiter and Saturn<sup>20,21</sup> where the major atmospheric constituent is molecular hydrogen. Therefore it is desirable to remeasure the differential elastic-scattering cross sections to give a consistent data set for an extensive energy and angular range.

The present paper presents the results of an experiment in which the DCS of electrons elastically scattered from H<sub>2</sub> have been measured by a crossed-beam method. The energy and angular range covered were from 2.0 to 200 eV and from  $-96^\circ$  to  $+156^\circ$ , respectively. The present results have discriminated against the vibrational and rotational excitations because of the 60-meV energy resolution of the apparatus.

### II. APPARATUS AND PROCEDURE

The apparatus used for the present measurements has been described in detail elsewhere.<sup>22,23</sup>

Briefly, it consists of three parts: a rotatable electron beam with the energy half-width of 60 meV, a neutral beam collimated by a capillary array, and a fixed detector system on the chamber wall. The stray magnetic fields have been reduced to less than 10 mG in all directions by three sets of Helmholtz coils. The absolute energy scale has been determined frequently by the He resonance at 19.3 eV within  $\pm 0.05$  eV.

The procedure used for the measurements was to integrate the signal of the electrons elastically scattered from the neutral beam for 10 sec at each angle and each electron energy. The angular range of  $-96^\circ$  to  $+156^\circ$  was scanned in  $12^\circ$  increments. Additional measurements were made at  $\pm 6^\circ$ ,  $18^\circ$ , and  $30^\circ$  for impact energies greater than 30 eV. The measurements were repeated with the H<sub>2</sub> beam off to obtain the background signal. The signal difference between the neutral beam on and off is the DCS of electrons elastically scattered from H<sub>2</sub> beam. When the neutral H<sub>2</sub> beam is on, the collimated beam density in the interaction region was approximately three times larger than the overall background.

Since the full width at half maximum of the collimated neutral beam, as shown in the previous paper (Ref. 22, Fig. 4), is well inside the field of view of the detector ( $\pm 4^\circ$ ) and the half-width of the focused electron beam ( $\pm 2^\circ$ ) is inside the collimated neutral beam, the path-length correction for the crossed-beam part is expected to be very small except for very small angles ( $< 10^\circ$ ). The volume correction (path length) due to the background density for the final data has been made, i.e., the signal from the background density has been measured to be  $(33 \pm 1)\%$  of the total signal at  $90^\circ$  after the neutral beam was displaced from the interaction region. As described previously,<sup>23</sup> the conventional  $\sin\theta$  correction has been applied to the static gas part of the signal which may cause an uncertainty in the differential cross sections below  $12^\circ$  as Trajmar *et al.*<sup>24</sup> have pointed out.

The present results have been calibrated among the incident energies by normalizing the scattered signal against the incident electron current and the target gas density at  $36^\circ$  and  $60^\circ$  where the contributions from the vibrational and rotational excitations are negligible (1%). The incident electron current is the saturated collected current which has been determined by increasing collector voltage in the Faraday cup which consists of a wide collecting plate without an entrance slit and a grounded screen in front of the plate located approximately

20 cm away from the interaction regions. The rotatable electron-beam source can be focused for all electron energies by use of an electron lens system.

The energy analyzer in the detector system has two electron lens systems that can focus the electrons before and after the energy analysis as well as a capability to decelerate and accelerate the electrons to maintain a constant energy resolution before and after the energy analysis. These electron lens systems and the decelerating (accelerating) system alter the transmission of electrons depending upon the energy. Therefore, it is necessary to detect the scattered signals without use of these lens systems and of decelerating and accelerating mechanisms in order to ensure a constant transmission of the detector. This has been confirmed experimentally in the following way. The transmission of the electron current has been determined by measuring the saturated currents of two collecting plates, one after the entrance slit and another after the exit slit of the energy analyzer in the detector system. The ratio of the two saturated currents stay the same to within 5% for energies down to 5.0 eV. The transmission at 2 eV is about 10% less than the constant for higher energies.

The relative elastic-scattering cross section of H<sub>2</sub> at 10 eV was normalized to that of He at 10 eV which has been normalized to that calculated by LaBahn and Callaway<sup>25</sup> (and Nesbet<sup>26</sup>). Static-gas experiments for both gases (H<sub>2</sub> and He) have been performed in the intergas normalization as follows. First, the whole scattering chamber was filled with the experimental gas at  $2 \times 10^{-5}$  torr after the neutral beam collimator was displaced from the interaction region and also the pumping speed for the system was reduced so that a uniform density was established throughout the scattering chamber. At this pressure in the chamber, there is no multiple scattering taking place because the mean-free path of electrons is larger than 10 m while the distance between the interaction region and the detector is 12 cm, approximately. When the experimental gas was on and off, the strength of the incident electron beam had been monitored constantly by two Faraday cups. A Faraday cup which covers an extensive angular range ( $30^\circ - 160^\circ$ ) also monitored the electron beam strength during the angular scan. The absolute pressure for both target gases were measured by a Bayard-Alpert ionization gauge which was calibrated by an MKS Baratron pressure meter within 5%. Thus the present results have been placed on an absolute scale.

TABLE I. Angular distribution,  $d\sigma/d\Omega$  in units of  $10^{-18} \text{ cm}^2/\text{sr}$  (parentheses are extrapolated data points).

$\theta^\circ/E$ (eV)	2	3	5	7	10	15	20	30	40	60	100	150	200
6													
12	107.6	182.3	336.2	340.3	375.0	384.2	337.6	365.0	342.1	245.5	207.1	175.8	124.1
18													
24	97.9	155.2	264.4	288.3	290.0	253.3	210.0	137.3	160.1	98.3	57.8	37.4	31.9
30													
36	92.5	125.1	201.5	210.2	200.5	163.4	126.0	68.6	48.2	25.2	12.4	7.9	5.6
48	78.5	102.7	154.3	157.9	141.5	101.8	75.3	36.7	25.3	11.6	5.0	2.65	1.97
60	67.8	89.7	120.6	117.9	109.0	65.2	44.7	21.5	13.5	5.8	2.5	1.39	1.08
72	64.5	79.0	97.6	88.8	79.4	43.1	27.9	13.0	8.4	3.2	1.5	0.85	0.75
84	73.2	74.7	85.1	70.3	59.7	28.8	18.0	8.4	5.4	1.95	1.03	0.59	0.44
96	88.2	78.5	73.9	62.5	47.0	21.2	12.6	5.9	3.8	1.41	0.71	0.46	0.28
108	109.7	100.4	90.2	61.3	41.8	17.0	9.9	4.6	3.0	1.12	0.66	0.36	0.22
120	140.8	132.8	100.7	66.0	40.9	15.3	8.7	3.9	2.1	1.08	0.57	0.31	0.19
132	170.0	156.3	120.6	74.3	42.4	15.1	8.7	3.9	1.9	1.00	0.53	0.23	0.15
144	205.4	190.6	140.9	89.6	46.0	16.0	8.9	3.9	1.8	1.04	0.50	0.17	0.12
156	237.1	233.6	156.7	97.8	46.9	16.4	9.0	4.0	1.9	1.08	0.46	0.15	0.11
168	(269.0)	(276.7)	(164.1)	(102.9)	(47.8)	(17.0)	(9.3)	(4.1)	(2.2)	(1.12)	(0.41)	(0.13)	(0.10)
$\sigma_{el}^a$	14.4	15.8	15.9	13.58	11.29	7.55	5.61	3.36	2.5	1.27	0.77	0.50	0.39
$\sigma_{MT}^a$	17.1	17.0	14.0	10.14	7.07	3.29	2.11	1.02	0.64	0.29	0.15	0.083	0.060

<sup>a</sup> $\sigma_{el}$  and  $\sigma_{MT}$  in units of  $10^{-16} \text{ cm}^2$ .

### III. EXPERIMENTAL RESULTS

DCS have been measured at each of 14 impact energies (2.0, 3.0, 5.0, 7.0, 10, 15, 20, 25, 30, 40, 60, 100, 150, and 200 eV). They are shown in Table I along with the total elastic-scattering and momentum-transfer cross sections.

The standard deviation in data points at each angle is less than 3% except for the large angles ( $> 120^\circ$ ) at the high energies ( $> 100$  eV) where the uncertainty is less than 5%. The uncertainties are less than 7% in the calibration process which consists of five sets of runs among the incident energies and 8% in the four normalization runs between He and H<sub>2</sub>. The volume correction (path length) contains  $\pm 2\%$  uncertainty and the adopted value of He at 10 eV has  $\pm 3\%$  uncertainty. Therefore the resultant uncertainty (in the mean-square root) for the present results is  $\pm 13\%$  except for  $6^\circ$  and  $12^\circ$  where the uncertainties are estimated to be less than 20%.

Figure 1 shows the DCS at 2.0 eV along with the results of Linder and Schmidt<sup>14</sup> and the theoretical calculation of Hara<sup>6</sup> at 2.5 eV. There is good agreement between the results of Linder and Schmidt and the present results for the shape and after the energy adjustment for the magnitude. It should be noted that the Linder and Schmidt measurements were normalized to the total cross section measured by Golden *et al.*<sup>15</sup> The results of Hara's calculation (case D in his paper) agree very well with the present results in shape and magni-

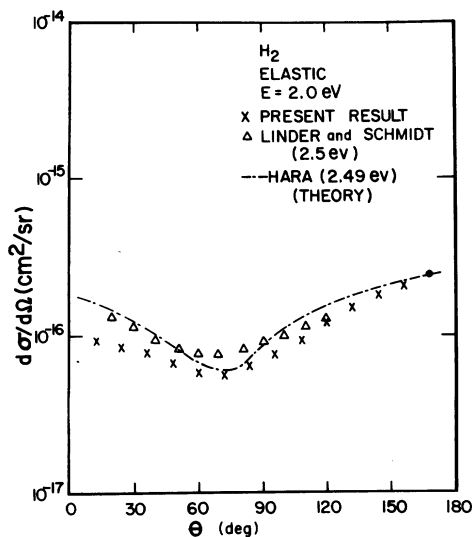


FIG. 1. DCS of 2.0-eV electron impact. Dot is an extrapolated data point.

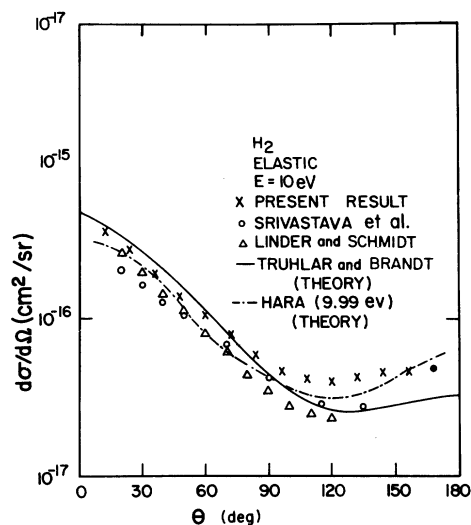


FIG. 2. DCS of 10-eV electron impact. Dot is an extrapolated data point.

tude after the energy adjustment.

Figure 2 shows the DCS at 10 eV along with other experimental and theoretical results. Hara's calculation is again in good agreement in shape with the present results, but the magnitude tends to be smaller. The theoretical results of Truhlar and Brandt<sup>11</sup> (potential 3 in their paper) are in relatively good agreement with the present results in the forward direction but have smaller values at large angles ( $> 90^\circ$ ). The revised results of Srivastava *et al.*<sup>13</sup> are systematically smaller than the present

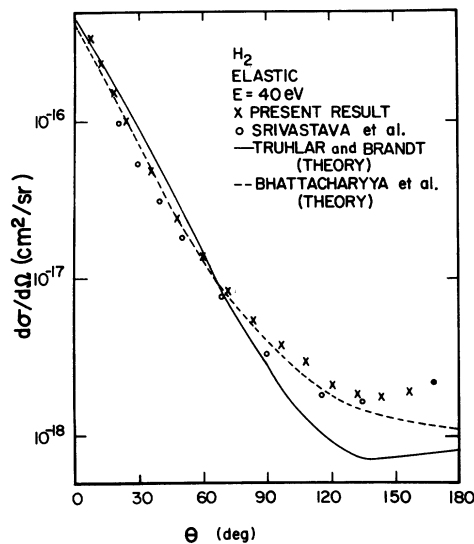


FIG. 3. DCS of 40-eV electron impact. Dot is an extrapolated data point.

results. The results of Linder and Schmidt are in good agreement with the present results in shape in the forward direction. There is a trend to smaller values in the backward scattering than the present results would indicate.

Figure 3 shows the DCS at 40-eV impact energy along with the revised measurements by Srivastava *et al.* which agree very well in shape with the present results but again are systematically smaller in magnitude. The theoretical value of Truhlar and Brandt<sup>11</sup> show slightly stronger forward and much weaker backward scattering than the present results. The theoretical results of Bhattacharyya and Ghosh<sup>10</sup> agree very well with the present results in the forward direction. Their results tend to smaller values than the present results as the angle increases.

Figures 4 and 5 show DCS at 100 and 200 eV along with other experimental results and theoretical results of Khare and Shobha.<sup>4</sup> The experimental results of Wingerden *et al.*<sup>17</sup> and Fink *et al.*<sup>16</sup> are in good agreement with the present results at energies of 100 and 200 eV. The results of Fink *et al.*<sup>16</sup> tend to underestimate the backward scattered component for 200 eV. The theoretical results of Khare and Shobha<sup>4</sup> are in good agreement with the present results for both energies, however, they underestimate the contribution at larger scattering angles ( $> 90^\circ$ ).

Figure 6 shows the total elastic-scattering cross sections deduced from this data along with other measurements and theoretical values calculated by a number of investigators. Within the accuracy of the present results the peak in the cross section is near 4 eV. The total cross section measured by Golden *et al.*<sup>15</sup> peaks near 3 eV and falls below the present results above this energy by about 15%. The revised values of Srivastava *et al.*<sup>13</sup> also maximize near 3 eV and are in relatively good agreement with the present results above 15 eV. The theories developed by Hara<sup>6</sup> and Henry and Lane<sup>9</sup> for scattering at energies less than 20 eV give good agreement with the present data. However, they tend to be near the upper limit on the experimental accuracy at 2 eV. The calculations by Truhlar and Brandt<sup>11</sup> predict the experimental results accurately. The calculations of Bhattacharyya *et al.*<sup>12</sup> decrease less rapidly above 25 eV than do the data.

Finally, Fig. 7 shows the moment-transfer cross sections,  $\sigma_{MT}$  that were calculated directly from the angular distributions by the equation,

$$\sigma_{MT} = \int_{\Omega} \frac{d\sigma}{d\Omega} (1 - \cos\theta) d\Omega,$$

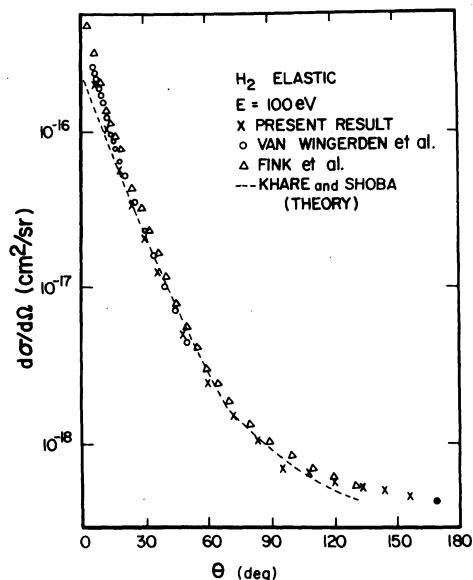


FIG. 4. DCS of 100-eV electron impact. Dot is an extrapolated data point.

along with the results of swarm experiments by Frost and Phelps,<sup>18</sup> Crompton *et al.*,<sup>19</sup> and the experiment of Srivastava *et al.*<sup>13</sup> The results of swarm experiments are in good agreement with the present results below 7 eV. Above 7 eV, these results are larger than the present results by as much as a factor of 2. It should be noted that

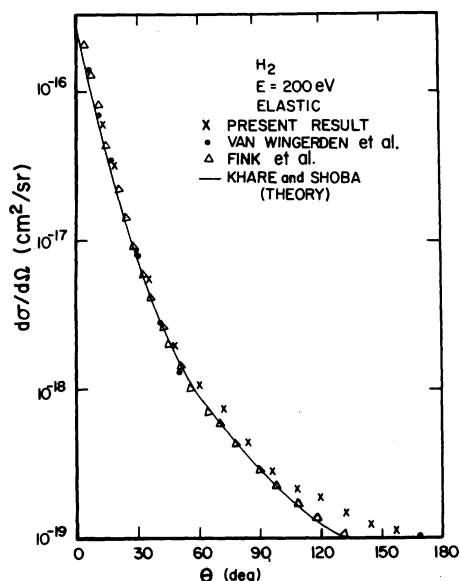


FIG. 5. DCS of 200-eV electron impact. Dot is an extrapolated data point.

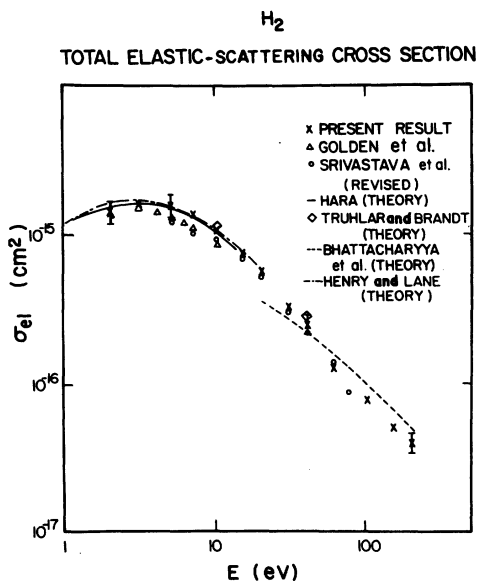


FIG. 6. Total elastic-scattering cross sections  $\sigma_{el}$ .

momentum-transfer cross sections derived from transport coefficients in swarm experiments depend strongly upon the assumptions used in the derivation. The results of Srivastava *et al.*<sup>13</sup> do not agree very well with the present results below 10 eV, however, their results are in good agreement with the present result above 10 eV.

#### IV. DISCUSSION

As shown in Sec. III, the results of Hara's calculation,<sup>6</sup> in which the static-exchange and the adiabatic dipole polarization potential have been used, agree in shape as well as magnitude within the experimental uncertainty with the present results below 10 eV. The theoretical results of Bhattacharyya and Ghosh,<sup>10</sup> Truhlar and Brandt,<sup>11</sup> and Bhattacharyya *et al.*<sup>12</sup> are in good agreement in the forward scattering ( $> 90^\circ$ ) with the present results but they have a general tendency to show significantly smaller DCS at large scattering angles than the present results by as much as a factor of 2 between 10 eV and 100 eV. This maybe, as Bhattacharyya and Ghosh<sup>10</sup> have pointed out, due to the lack of an accurate knowledge of the potential in the short-range interaction (small- $r$  interaction) region which contributes mainly to the large-angle scattering. The short-range interaction includes

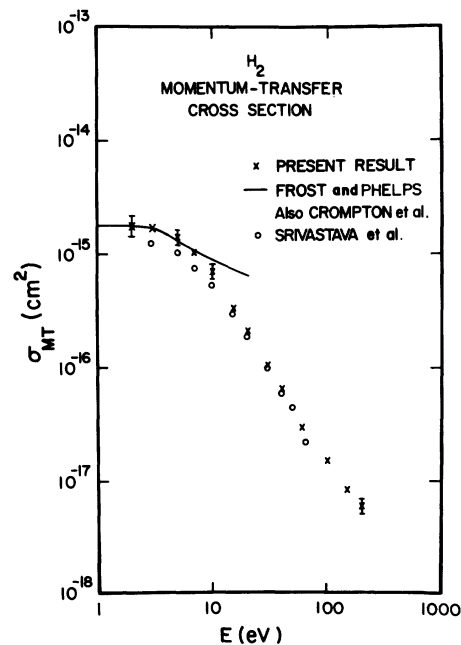


FIG. 7. Momentum-transfer cross section  $\sigma_{MT}$ .

the nonspherical part of the potential which is expected to play a significant role for the large-angle scattering.

The total elastic-scattering cross section calculated theoretically agrees with the present results even though there is a significant disagreement in DCS at large angles. This is due to the  $\sin\theta$  factor used in the integrations of DCS over angles to get the total elastic-scattering cross section. That is to say, there is agreement in the total elastic-scattering cross section generally when the DCS agree near  $90^\circ$ . However, it should be noted that the DCS is the more fundamental physical quantity to test the theory because several nonunique DCS can lead to the same total elastic-scattering cross section after the integration over angles.

#### ACKNOWLEDGMENTS

This work was supported by NSF under Grant No. ATM79-01618. The authors thank Winston Chang for his help in taking and analyzing the data.

- <sup>1</sup>D. E. Golden, N. F. Lane, A. Temkin, and E. Gerjuoy, *Rev. Mod. Phys.* **43**, 642 (1971).
- <sup>2</sup>N. F. Lane, *Rev. Mod. Phys.* **52**, 29 (1980).
- <sup>3</sup>P. Gupta and S. P. Khare, *J. Chem. Phys.* **68**, 2193 (1978).
- <sup>4</sup>S. P. Khare and S. Shobha, *J. Phys. B* **7**, 420 (1974).
- <sup>5</sup>S. S. Dhal, B. B. Srivastava, and R. Shingal, *J. Phys. B* **12**, 2211 (1979).
- <sup>6</sup>S. Hara, *J. Phys. Soc. Jpn.* **27**, 1009 (1969).
- <sup>7</sup>B. I. Schneider, *Phys. Rev. A* **11**, 1957 (1975).
- <sup>8</sup>N. F. Lane and S. Geltman, *Phys. Rev.* **184**, 46 (1969).
- <sup>9</sup>R. J. W. Henry and N. F. Lane, *Phys. Rev.* **183**, 221 (1969).
- <sup>10</sup>P. K. Bhattacharyya and A. S. Ghosh, *Phys. Rev. A* **12**, 480 (1975).
- <sup>11</sup>D. G. Truhlar and M. A. Brandt, *J. Chem. Phys.* **65**, 3092 (1976).
- <sup>12</sup>P. K. Bhattacharyya, K. K. Goswami, and A. S. Ghosh, *Phys. Rev. A* **18**, 1865 (1978).
- <sup>13</sup>S. K. Srivastava, A. Chutjian, and S. Trajmar, *J. Chem. Phys.* **63**, 2659 (1975).
- <sup>14</sup>F. Linder and M. Schmidt, *Z. Naturforsch.* **26a**, 1603 (1971).
- <sup>15</sup>D. E. Golden, H. W. Bandel, and J. A. Salerno, *Phys. Rev.* **146**, 40 (1966).
- <sup>16</sup>M. Fink, K. Jost, and D. Herrmann, *Phys. Rev. A* **12**, 1374 (1975).
- <sup>17</sup>B. Van Wingerden, E. Weigold, F. J. de Heer, and K. J. Nygaard, *J. Phys. B* **10**, 1345 (1977).
- <sup>18</sup>L. S. Frost and A. V. Phelps, *Phys. Rev.* **127**, 1621 (1962).
- <sup>19</sup>R. W. Crompton, D. K. Gibson, and A. I. McIntosh, *Aust. J. Phys.* **22**, 715 (1969).
- <sup>20</sup>J. H. Waite, Jr., Ph.D. thesis, University of Michigan, 1980 (unpublished).
- <sup>21</sup>J. H. Waite, Jr., T. E. Cravens, S. K. Atreya, J. Kozyra, and A. F. Nagy, *EOS Trans. Am. Geophys. Union* **61**, 1024 (1980).
- <sup>22</sup>T. W. Shyn, R. S. Stolarski, and G. R. Carignan, *Phys. Rev. A* **6**, 1002 (1972).
- <sup>23</sup>T. W. Shyn, *Phys. Rev. A* **22**, 916 (1980).
- <sup>24</sup>S. Trajmar, J. K. Rice, D. G. Truhlar, A. Kupperman, and R. T. Brinkmann, *Proceedings of the Sixth International Conference on the Physics of Electronic and Atomic Collisions*, edited by I. Amdur (MIT, Cambridge, Mass., 1969), p. 87.
- <sup>25</sup>R. W. LaBahn and J. Callaway, *Phys. Rev. A* **2**, 366 (1970).
- <sup>26</sup>R. K. Nesbet, *Phys. Rev. A* **20**, 58 (1979).